

1 **Inferred molecular bioavailability of pyrogenic organic matter**
2 **compared to natural organic matter from global sediments and**
3 **surface waters**

4
5 Emily B. Graham^{+,*} 1,2, Hyun-Seob Song^{+,3}, Samantha Grieger^{1,4}, Vanessa A. Garayburu-
6 Caruso^{1,5}, James C. Stegen¹, Kevin D. Bladon⁶, and Allison Myers-Pigg^{*,1,4}

7
8 ⁺equal contributors

9 ^{*}corresponding authors: emily.graham@pnnl.gov, allison.myers-pigg@pnnl.gov

10

11 ¹ Earth and Biological Sciences Directorate, Pacific Northwest National Laboratory, Richland,
12 WA, USA

13 ² School of Biological Sciences, Washington State University, Richland, WA USA

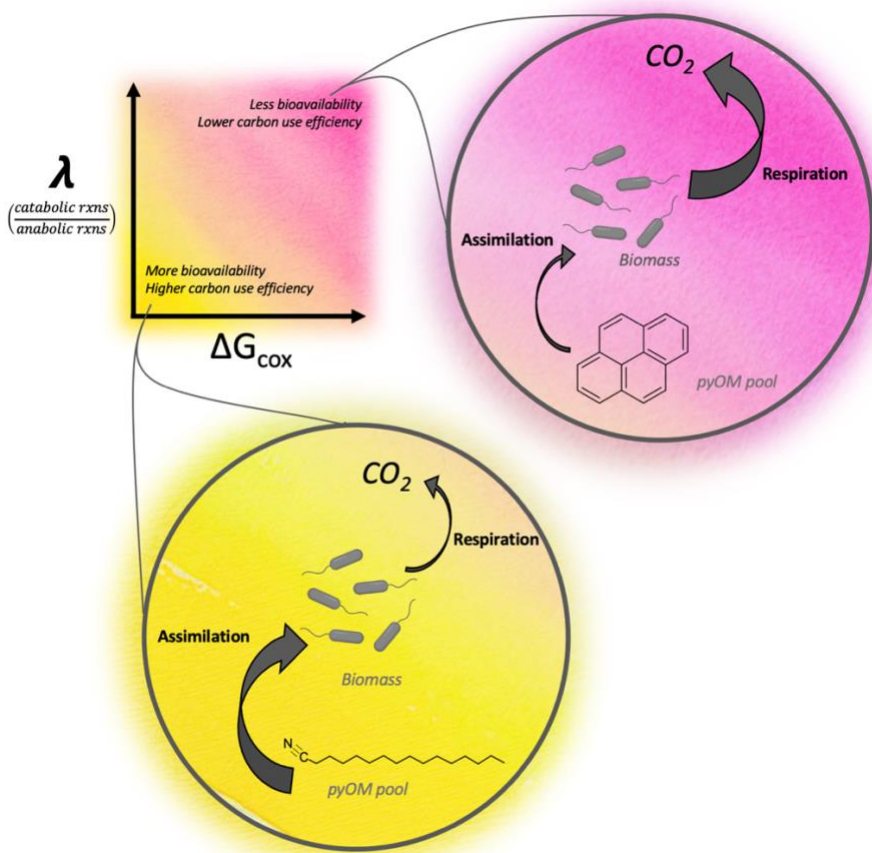
14 ³ Department of Biological Systems Engineering, Department of Food Science and Technology,
15 Nebraska Food for Health Center, University of Nebraska, Lincoln, NE, USA

16 ⁴ Marine and Coastal Research Laboratory, Pacific Northwest National Laboratory, Richland,
17 WA, USA

18 ⁵ School of the Environment, Washington State University, Richland, WA USA

19 ⁶ College of Forestry, Oregon State University, Corvallis, OR, USA

20 GRAPHICAL ABSTRACT



21

22

23 ABSTRACT

24 Pyrogenic materials generated by wildfires are transported across terrestrial landscapes
25 into inland waters, creating many consequences for aquatic ecosystems. At least ~10% of
26 dissolved organic matter pools may be comprised of pyrogenic organic matter (PyOM), but
27 heterogeneous PyOM chemistry complicates efforts to understand its bioavailability. We used a
28 substrate-explicit model to predict the energy content, metabolic efficiency, and rate of aerobic
29 decomposition of representative PyOM compounds from primary literature. This enabled us to
30 systematically evaluate the bioavailability of a full spectrum of PyOM chemistries – which
31 would be unfeasible with laboratory experiments – and compare it to measured natural organic
32 matter (NOM) pools from global aquatic ecosystems. Overall, we found the range of predicted
33 bioavailability of PyOM was similar to NOM. Thermodynamic properties and carbon use
34 efficiencies of PyOM and NOM were statistically indistinguishable. Within PyOM, phenolic and
35 BC molecules had lower metabolic efficiency than other PyOM and NOM compounds, and the
36 impact of oxygen limitation on BC metabolism was lower than for other PyOM classes. In total,
37 our work supports the recent paradigm shift regarding PyOM bioavailability, highlighting its
38 potential role in global C emissions as the prevalence of wildfires increases.

39 INTRODUCTION

40 Wildfires have burned an average of 1.8-million ha year⁻¹ in the US alone over the past
41 80 years¹ with dramatic impacts on terrestrial and aquatic ecosystem functions.²⁻⁵ The frequency,
42 extent, and severity of wildfire activity in many regions has increased rapidly in response to
43 pervasive hotter and drier conditions associated with climate change,⁶⁻⁹ a trend that is expected to
44 continue.¹⁰ The impact of wildfires on river corridor biogeochemistry has received significant
45 recent attention and is mediated by the loading of sediment and pyrogenic materials into
46 waterways.^{11, 12} In particular, pyrogenic organic matter (PyOM) is a complex continuum of
47 materials generated by thermal alteration of biomass^{13, 14} and can have substantial impacts on
48 river corridor biogeochemistry due to the importance of organic matter as a carbon (C) and
49 energy source in rivers. Globally, wildfires generate 116–385 Tg per year of the most commonly
50 measured constituent of PyOM—black carbon (BC, defined herein as the condensed aromatic
51 fraction of PyOM typically measured by benzene polycarboxylic acid (BPCA) method^{11, 15}). This
52 wildfire generated BC provides a continuous source of PyOM to inland waters that totals 300 to
53 500 giga-metric tons of C stored in sediments, soils, and waters.¹⁶⁻²⁰ Within river corridors, BC
54 alone constitutes ~10% of dissolved organic C pools.¹⁶ Given that organic matter drives
55 biogeochemical cycles in most aquatic ecosystems, the loading of PyOM into river corridors has
56 the potential to produce substantial impacts on ecosystem functions and downstream drinking
57 water treatability.^{21, 22}

58 Historically, PyOM has been considered refractory, passively transported and deposited
59 throughout landscapes. Some estimates of PyOM residence times in aquatic landscapes extend
60 thousands of years.²³⁻²⁶ Yet, simple mass balances suggest depositional reservoirs, including soils
61 and sediments, do not fully account for PyOM production via biomass burning.²⁷ This implies

62 biotic and/or abiotic loss from source to sink.²⁸ This paradigm shift is highlighted by recent work
63 that has shown PyOM may be more bioavailable than previously thought²⁹⁻³¹, and is also
64 supported by biochar research highlighting a variety of reactivity of combustion by-products.^{32, 33}
65 PyOM may constitute a significant and unconstrained contributor to global biogeochemical
66 cycles and climate feedbacks. To address this knowledge gap, we used a substrate-explicit model
67 to predict organic matter energy content, metabolic efficiency, and rate of aerobic decomposition
68 to compare the bioavailability of PyOM to natural organic matter (NOM) in global surface
69 waters and sediments. We hypothesized that the continuum of chemistries in PyOM would show
70 roughly comparable bioavailability to diverse NOM pools.

71 We leverage a newly developed substrate-explicit model³⁴ that parameterizes OM-
72 specific oxidative degradation pathways and reaction rates based on the thermodynamic
73 properties of OM molecules. It relies on the elemental composition of individual OM molecules
74 to provide a systematic way to formulate reaction kinetics and enable flexible application across
75 environments, as it is agnostic of many factors that have complicated a universal understanding
76 of OM bioavailability, including molecular structure (e.g., double bonding and aromatic rings),
77 priming dynamics, chemical inhibition, mineral-associations and physical protection, terminal
78 electron acceptor concentrations, microbial community composition and accessibility, and
79 abiotic reactions (reviewed in Arndt et al.³⁵). The model requires two simple parameters (U_{max}
80 and V_h , see Supporting Information), which focus on the chemical composition of OM as a
81 governing factor in metabolism and overcome a key limitation in modelling aquatic OM
82 decomposition, that variation in parameters across environments limits transferability of model
83 predictions.³⁵ This ecosystem-agnostic approach allows us to examine the molecular
84 bioavailability of individual OM molecules, and it provides a baseline for future work

85 investigating pool-scale dynamics that require a broader range of parameters calibrated for
86 environmental context and targeted laboratory experiments that a examine the bioavailability of a
87 narrower range OM across environmental contexts. In total, our results support an emerging
88 paradigm in wildfire science in which PyOM are more bioavailable than historically considered.

89

90 **MATERIALS AND METHODS**

91 An extended version of our methods is available in the Supporting Information.

92 To assess the bioavailability of PyOM, we searched primary literature for representative
93 compounds of the PyOM continuum. Specifically, we targeted characteristic organic compounds
94 from field and laboratory burns of various fuel types representing a range of moisture,
95 temperature, and oxygen conditions (Table S1). The chosen compounds focused on biomass
96 burning alteration products, which are often used to characterize PyOM in the environment. This
97 included compounds such as theoretical BC compounds (defined here as condensed aromatic
98 core structures polysubstituted with O-containing functionalities³⁶), anhydrosugars, and
99 polycyclic aromatic hydrocarbons (PAHs). The list also included compounds created and/or
100 transformed from biomass burning, such as those derived from biopolymers like lignin (e.g.,
101 methoxyphenols), waxes (e.g., n-alkenes from thermal dehydration of n-alkanols), and resins
102 (e.g., thermally oxidized diterpenoids).^{37, 38} In total, our literature search for PyOM chemistries
103 yielded 389 compounds with 207 unique chemical formulae.

104 After generating a set of representative compounds, we used a substrate-explicit
105 modelling framework developed by Song et al.³⁴ to characterize the bioavailability of each
106 compound and predict its rate of decomposition. Importantly, the model utilizes molecular
107 formulae to predict energetic content, metabolic efficiency, and rates of aerobic metabolism,

108 while it does not account for structural components of organic molecules (e.g., double bonds,
109 folding patterns, cross-linkages). This enabled flexibility in application to high-throughput mass
110 spectrometry techniques that yield chemical formulae but not structural information (e.g., Fourier
111 Transform Ion Cyclotron Resonance Mass Spectrometry, FTICR-MS). Despite its limitations,
112 the substrate-explicit model used here has proven useful in linking NOM composition to aerobic
113 metabolism in natural environments^{34, 39, 40}, and its structure is consistent with Harvey et al.⁴¹
114 who argued for the importance of thermodynamic estimates of PyOM bioavailability that
115 underlie this model. It was chosen to allow for comparison of PyOM to the most comprehensive
116 assessment of global aquatic NOM pools to date.⁴²

117 Briefly, the substrate-explicit model uses the elemental stoichiometry of organic
118 molecules, based on molecular formulae, to predict the number of catabolic reactions that must
119 occur to provide the energy required for the synthesis of one mole of biomass carbon. This
120 quantity is described by the parameter lambda (λ) in which lower λ values denote more efficient
121 energetics of catabolism in producing biomass through anabolism. The model also predicts the
122 Gibbs free energy of C oxidation (ΔG_{Cox}), under standard conditions with a modification to pH 7
123 adjusted from LaRowe and Van Cappellen⁴³ by Song et al.³⁴, as well as C use efficiency (CUE)
124 as defined by Saifuddin et al.⁴⁴ Lower ΔG_{Cox} denotes higher thermodynamic favorability in an
125 electron donor half reaction associated with organic matter, and higher CUE reflects more C
126 assimilated into biomass per unit C respired. We also predicted the rate of aerobic metabolism
127 (as oxygen consumed per mol-C biomass produced) under three scenarios commonly observed in
128 aquatic ecosystems: (a) C-limitation, (b) oxygen (O_2) limitation, and (c) both C and O_2 -
129 limitation. For more details of the substrate-explicit modelling approach used, please see Song et
130 al.³⁴ Each metric (λ , ΔG_{Cox} , CUE, metabolic rates) denotes a different aspect of bioavailability.

131 Though the relative magnitude of the metrics in comparison to each other will vary based on the
132 specific stoichiometry of a molecule, highly bioavailable compounds are indicated by low λ and
133 ΔG_{Cox} coinciding with high CUE and metabolic rates.

134 Three sets of organic molecules were used as model inputs: global dissolved (1) surface
135 water NOM and (2) sediment NOM pools, measured by FTICR-MS as described by Garayburu-
136 Caruso et al.⁴²; and (3) literature-derived PyOM compounds as described above. Inputs to the
137 model from the PyOM compounds were unique molecular formulae, grouped in subsequent
138 analysis by their corresponding compound classes (Table S1). If one molecular formula was
139 represented by several PyOM compounds (e.g., $C_{10}H_{16}O_2$, which corresponds to the
140 sesquiterpenoid cis-Thujan-10-oic acid and 3-, 4- substituted methylcatechol phenols), we
141 assigned multiple compound classes to that molecular formula. Surface water and sediment
142 NOM pools were filtered to compounds occurring in 95% of samples to yield a dataset of
143 globally ubiquitous NOM. Formulae assignment and inferred chemical classes via Van Krevelen
144 diagrams in NOM pools are described by Garayburu-Caruso et al.⁴² We compared modelling
145 outputs from representative PyOM to outputs of ubiquitous NOM pools to infer relative
146 bioavailability using ANOVA and Tukey HSD statistical tests with R software. All model
147 outputs are available in Tables S2-S4. Code is available at:
148 <https://github.com/hyunseobsong/lambda>. Data describing NOM pool chemistry are published as
149 a data package⁴⁵ (available at: doi:10.15485/1729719) and are discussed in more detail by
150 Garayburu-Caruso et al.⁴².

151

152 **RESULTS AND DISCUSSION**

153 We used a substrate-explicit model to evaluate the emerging paradigm of PyOM
154 bioavailability and compared model outputs to comprehensive measurements of global NOM
155 pool composition.^{34, 39, 40, 42} In contrast to previous characterizations of PyOM bioavailability,^{29,}
156 ^{30, 41, 46} the model-based approach enabled us to directly compare known combustion products to
157 thousands of ubiquitous NOM compounds, which would have been unfeasible to directly assess
158 in a laboratory setting.

159

160 *Inferred Molecular Bioavailability of Pyrogenic Organic Matter.*

161 Though previous work has shown that OM chemistry of sediment and surface waters is
162 altered by wildfires,^{11, 16, 47, 48} our results suggest that the chemically distinct pools of OM altered
163 by pyrolysis may have similar overall bioavailability to NOM. We found that the ranges of
164 ΔG_{Cox} , λ , and CUE were similar between PyOM and NOM pools in sediments and surface
165 waters (Figure 1 and 2a). Predicted CUE of PyOM classes was also comparable to literature
166 values reported by others.^{44, 49, 50} Similarly, λ did not vary across all groups of organic molecules
167 or in post-hoc pairwise comparisons (ANOVA $p = 0.09$, and Tukey HSD p (PyOM-sediment) =
168 0.92, p (PyOM-water) = 0.40, p (water-sediment) = 0.10). While ΔG_{Cox} and CUE were
169 significantly different when comparing all three groups (ANOVA, $p < 0.001$), surface water and
170 sediment NOM had greater dissimilarity in these parameters than any comparison involving
171 PyOM. For example, the mean difference in NOM between surface water and sediment was 7.34
172 kJ/mol-C for ΔG_{Cox} and 0.058 for CUE. Comparatively, the differences between PyOM and both
173 surface water and sediment were less than 7.4 kJ/mol-C for ΔG_{Cox} and 0.058 for CUE. Further,
174 there was no evidence that CUE was different between PyOM and sediment NOM (Tukey HSD,
175 $p = 0.20$). These results signal a strong overlap between PyOM bioavailability and NOM pools;

176 however, within PyOM compounds, there was variability in ΔG_{Cox} , λ , and CUE consistent with a
177 heterogeneous continuum of organic matter (Figure 1 and S1). This is not surprising, given the
178 diversity of PyOM chemistries generated by wildfires of different burn severities and source
179 materials,^{11, 51, 52} some of which overlap with chemical classes in unaltered NOM.

180 Interestingly, the relative equivalence of predicted CUE across PyOM and NOM pools
181 revealed that PyOM decomposition in rivers could emit comparable amounts of CO₂ per mole of
182 C to extant NOM pools. CUE is used in many microbially-explicit decomposition models to
183 constrain organic matter bioavailability,⁵³⁻⁵⁹ and predicted CUE from PyOM pools can be easily
184 assimilated in microbially-explicit model predictions that rely on CUE as an input parameter.
185 Such an approach could be used to directly evaluate the impact of PyOM on global C cycles,
186 leading to a better incorporation of PyOM impacts in model predictions.⁶⁰

187 Within PyOM (Figure 1c), two clusters of compounds were distinctly separated from the
188 energetic and metabolic properties of most PyOM. For example, phenols had greater λ values
189 than the majority of PyOM and NOM compounds (all $\lambda > 0.039$, mean $\lambda = 0.084$), while the
190 electron donor half reaction involving BC molecules were less energetically favorable than other
191 PyOM classes (all $\Delta G_{Cox} > -143.42$, mean $\Delta G_{Cox} = -136.40$). However, both were within the
192 range of variability in NOM pools (Figure 1). Phenols and BC also had among the lowest CUE
193 values (BC mean = 0.47 and phenols mean = 0.54). Phenols are traditionally associated with
194 refractory organic matter, such as lignin and tannins, that exhibit long residence times in soils,⁶¹
195 although they have also been reported to be bioavailable in soils and waters in recent years (e.g.,
196 ^{61, 62}). Additionally, BC in this study is defined by inferred aromaticity from ultrahigh resolution
197 mass spectroscopy (i.e., the presence of condensed aromatic structures), which is also considered
198 to have low reactivity.^{26, 36} Although the bioavailability of the phenols and BC classes is

199 consistent with traditionally defined refractory PyOM pools, it is within the bioavailability range
200 observed in NOM, and these compound classes represent only a small portion of the PyOM
201 continuum.^{11, 14} We note that the comparatively low predicted CUE of phenols and BC indicates
202 that, if metabolized, their decomposition could have a greater impact on river corridor CO₂
203 emissions than other PyOM and NOM compounds. As a result, current understanding may
204 substantially underestimate the size, reactivity, and hydrobiogeochemical role of PyOM.¹¹

205

206 *Inferred Metabolism of Pyrogenic Organic Matter.*

207 Predicted rates of PyOM metabolism were also similar to NOM pools (Figure 2b),
208 reinforcing comparable bioavailability between the two pools of organic matter. Pairwise
209 comparison of metabolic rates revealed no evidence for differences between PyOM and sediment
210 NOM under oxygen limitation (Tukey HSD, $p = 0.23$) and without carbon or oxygen limitations
211 (Tukey HSD, $p = 0.34$). However, there was strong evidence that metabolic rates of both PyOM
212 and sediment NOM were different than surface water NOM (Tukey HSD, all $p < 0.001$). Aquatic
213 sediments can reach anoxia within millimeters of the sediment-water interface such that model
214 predictions under oxygen limitation may translate to no meaningful difference between PyOM
215 and NOM in natural sediments. Under C-limitation, PyOM had a statistically elevated rate of
216 metabolism relative to both surface water and sediment NOM (Tukey HSD, all $p < 0.001$).
217 However, we noted only small differences in rate values (means, surface water: 0.13, sediment:
218 0.13, PyOM: 0.17), with a similar range of values in sediment NOM (0.0008–0.45) and PyOM
219 (4.75e-08–0.45). Statistical differences were not surprising given an extremely large sample size
220 for NOM (sediment $n = 398$, surface water $n = 811$), and the low effect sizes denote that overall

221 differences in metabolisms between PyOM and NOM were minimal despite statistical
222 separation.

223 When considering the impact of various elemental limitations on PyOM metabolism, rate
224 predictions were strongly inhibited under low carbon and oxygen conditions. Predicted rates of
225 PyOM metabolism were approximately six times lower when C or O₂ was scarce. Low
226 decomposition rates such as those predicted here under oxygen and C limitation could be one
227 reason for the observed persistence of PyOM in depositional features that tend to be anoxic with
228 refractory C pools.²³⁻²⁵ Still, it is worthwhile to note that metabolism of all PyOM classes under
229 low O₂ or C was predicted to be substantially slower than without elemental limitations,
230 indicating PyOM compounds may both actively cycle in well-oxygenated surface waters with
231 fresh C inputs²⁸ and persist over long periods of time in O₂-limited sediments.

232 Among PyOM compound classes, BC was less negatively impacted by oxygen limitation
233 than any other group (Figure S2). Previous work has demonstrated that microorganisms are
234 capable of decomposing chemically complex organic molecules, such as long-chained and/or
235 aromatic hydrocarbons under low oxygen availability and/or anaerobia.⁶³⁻⁶⁶ Similar microbial
236 metabolic pathways may also be capable of degrading BC molecules in natural settings and
237 could be investigated with future laboratory work. Notably, our work also supports the notion
238 that black nitrogen could be more bioavailable than BC. We posit this may be due, in part, to its
239 chemical structure that includes pyrrole-type moieties, which are relatively biodegradable.^{67, 68}
240 While we only examined one class of PyOM molecules containing nitrogen (n-alkylnitriles), it
241 had among the highest predicted CUE and rates of aerobic metabolism.

242

243 *Correspondence to Empirical Investigations.*

244 While the substrate-explicit modelling approach used here has been validated in natural
245 settings and enabled comparison to a rich suite of ubiquitous NOM molecules, one key limitation
246 is its inability to account for structural characteristics of organic matter. Indeed, some aspects of
247 model predictions are inconsistent with experimental evidence, highlighting the role of
248 laboratory studies in evaluating PyOM bioavailability. For instance, n-alkenes and related
249 compounds tended to be most favorable for metabolism, despite these compound classes having
250 high stability in the environment and common usage as paleo-proxies in soils and sediments
251 (e.g., ^{69, 70}). These compounds are characterized by carbon-carbon double bond functional
252 groups, which may decrease bioavailability and are not considered in the model predictions.
253 Fatty acids and n-alkanes biomass burning by-products are generally reduced in chain length in
254 comparison to their un-burned counterparts⁷¹, and thus may be relatively bioavailable compared
255 to other lipids. Additionally, we note that previous work has shown fast degradation of
256 combustion-derived lipids in soils;⁷¹ as well as high n-alkene metabolism under anaerobic
257 conditions (in particular by sulfate-reducing bacteria⁷²⁻⁷⁵), n-alkene metabolism in natural
258 sediments,^{75, 76} and a range in lipid reactivities at the sediment-water interface.⁷⁷ While work on
259 n-alkene metabolism in aerobic settings is limited, the comparative bioavailability of n-alkenes
260 and known microbial degradation pathways suggests diverse microbiomes in sediments may
261 metabolize these compounds as part of natural biogeochemical cycles. Another notable
262 discrepancy is the relatively low bioavailability of anhydrosugars when compared to other PyOM
263 compounds. Experimentally, anhydrosugars are highly bioavailable in oxic conditions, with a
264 half-life of less than seven days.³⁰ The model may therefore not adequately account for enzyme-
265 catalyzed reactions, such as levoglucosan kinase or levoglucosan dehydrogenase, which cleave
266 and phosphorylate the 1,6-intramolecular linkage,⁷⁸ and could be potentially common enzymes

267 utilized by aquatic microorganisms.⁷⁹ Because of these nuances, the PyOM compound classes
268 presented here are best used as bounding estimates for experimental validation, and for holistic
269 comparison to NOM bioavailability. Still, the span of compounds investigated here, and their
270 comparison to NOM pools, provides a breadth of PyOM investigation that is unfeasible without
271 model-based approaches.^{29, 30, 41, 46}

272

273 *Conclusions.*

274 Our data supports the recent paradigm shift towards high PyOM bioavailability and
275 provides a foundation for detailed laboratory experiments investigating specific components of
276 the PyOM continuum. Intensifying wildfire regimes in many parts of the world are increasing the
277 production of PyOM with potential implications for source water supplies, which are critical for
278 domestic, industrial, agricultural, and ecological needs. Yet, many fundamental questions, such
279 as “how much” PyOM exists in ecosystems, “how fast” it cycles, and “how old” it is remain
280 largely unknown, and are an active area of research.⁸⁰ Furthermore, there has been no systematic
281 evaluation of the bioavailability of different constituents within the heterogeneous pools that
282 comprise the PyOM continuum.⁸¹ Our work provides the first comprehensive computational
283 assessment of the bioavailability of various chemical classes of PyOM in comparison to NOM
284 pools. The comparable bioavailability to NOM revealed that PyOM may be actively transformed
285 within the river corridor and may be an increasing source of C emissions to the atmosphere in the
286 future as the prevalence of wildfires increases.

287

288 **AUTHOR INFORMATION**

289

290 EBG conceived of the manuscript and was responsible for writing the manuscript and drafting all
291 figures. HSS performed all modelling. SG determined PyOM compounds for modelling based on
292 extensive literature review, with guidance from AMP. VGC and JCS contributed data and insight
293 on NOM pool chemistry. All authors contributed to revisions.

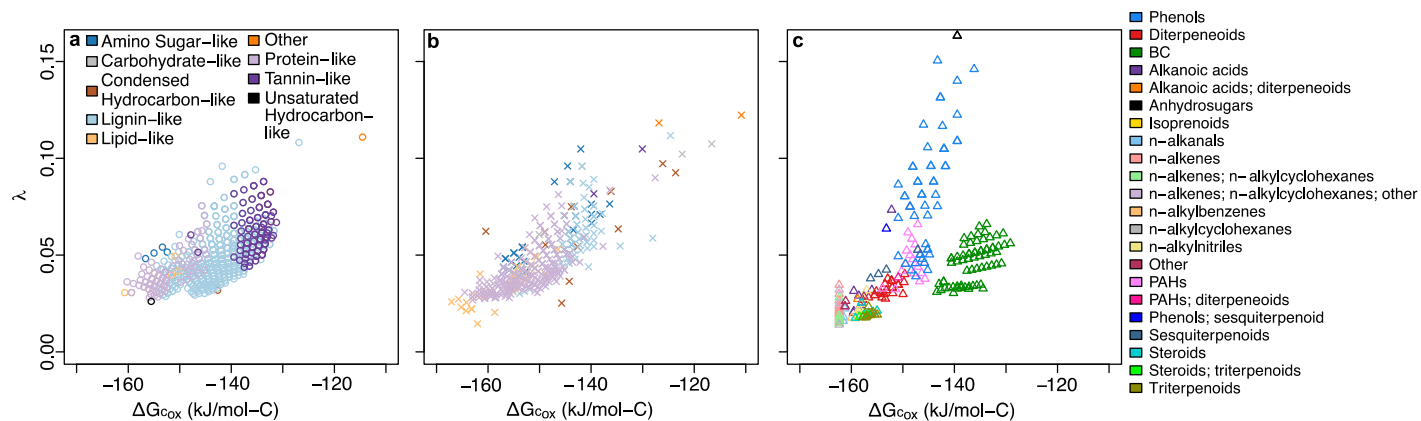
294

295 **ACKNOWLEDGMENTS**

296

297 This research was supported by the U.S. Department of Energy (DOE), Office of Biological and
298 Environmental Research (BER), Environmental System Science (ESS) Program as part of the
299 River Corridor Science Focus Area (SFA) at the Pacific Northwest National Laboratory (PNNL).
300 PNNL is operated by Battelle Memorial Institute for the U.S. Department of Energy under
301 Contract No. DE-AC05-76RL01830. This study used data from the Worldwide
302 Hydrobiogeochemistry Observation Network for Dynamic River Systems (WHONDRS) under
303 the River Corridor SFA at PNNL and facilitated by the U.S. Department of Energy
304 Environmental Molecular Science Laboratory User Facility.

305



306

307

308 **Figure 1.** Comparison of PyOM energy content (ΔG_{Cox}) and metabolic efficiency (λ) to global

309 NOM. Ubiquitous NOM molecules detected via FTICR-MS in global (a) surface water and (b)

310 sediment are colored by inferred chemical class. (c) Representative PyOM molecules are colored

311 by known chemical properties. Because PyOM molecules were derived from primary literature,

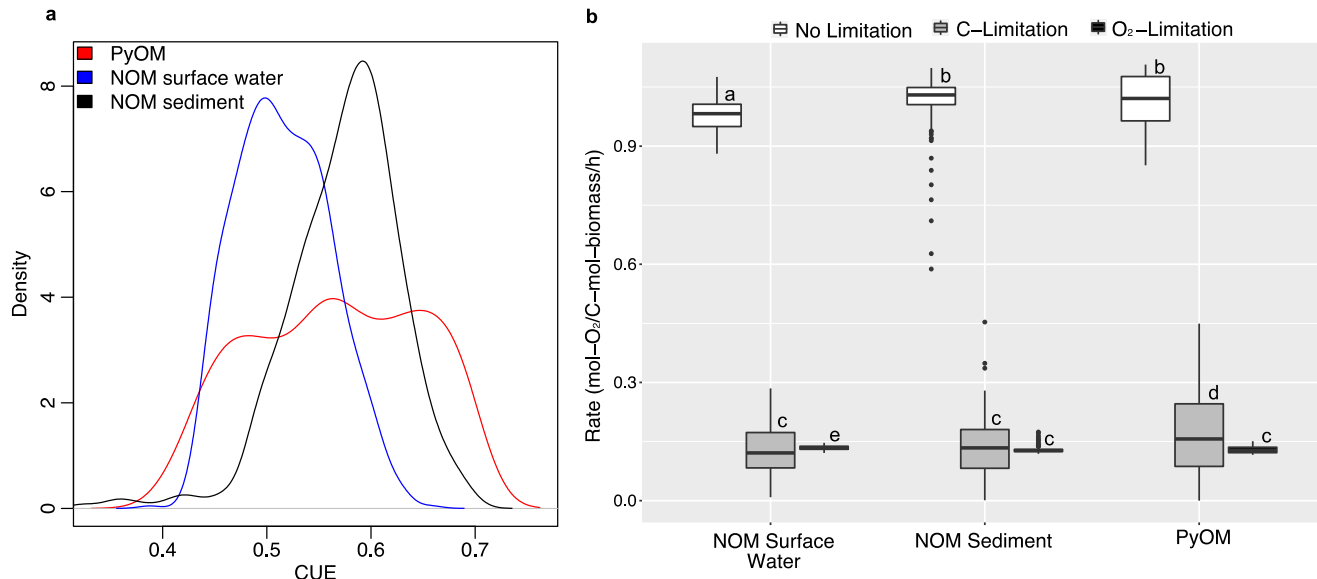
312 we are able to assign chemical properties at higher resolution than inferred classes from

313 measured NOM pools. Details on inferred chemical class assignment are provided in the

314 Supporting Information. Legends are inset in (a) for (a) and (b), and to the right of (c).

315

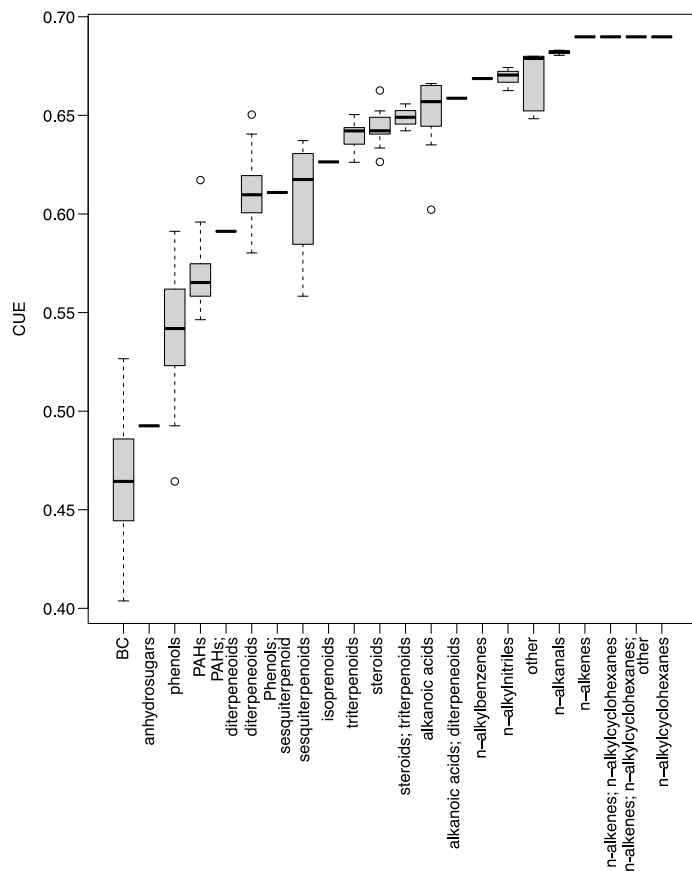
316



317

318 **Figure 2.** Carbon use efficiency (CUE) and predicted metabolism of NOM and PyOM. (a)
 319 shows the distribution of CUE in PyOM (red) and ubiquitous surface water (blue) and sediment
 320 (black) NOM molecules rates. It shows a probability density function (PDF) that reflects the
 321 relative likelihood that value of a random sample drawn from a particular group would equal the
 322 value on the x-axis. (b) depicts the predicted metabolism of surface water NOM, sediment NOM,
 323 and PyOM. Letters in (b) denote statistical groups. Median values are denoted by a bar, the
 324 lower and upper hinges correspond to the first and third quartiles (the 25th and 75th percentiles),
 325 and the upper and lower whiskers extend from the hinge to the largest/smallest value no further
 326 than 1.5 * IQR from the hinge (where IQR is the inter-quartile range, or distance between the
 327 first and third quartiles), and data beyond the end of the whiskers are plotted individually.

328 SUPPLEMENTAL FIGURES



329

330 **Figure S1.** Carbon use efficiency (CUE) of PyOM, grouped by known chemical properties. High

331 CUE values indicate more C incorporated into biomass vs. respired per unit C. Median values

332 are denoted by a bar, the lower and upper hinges correspond to the first and third quartiles (the

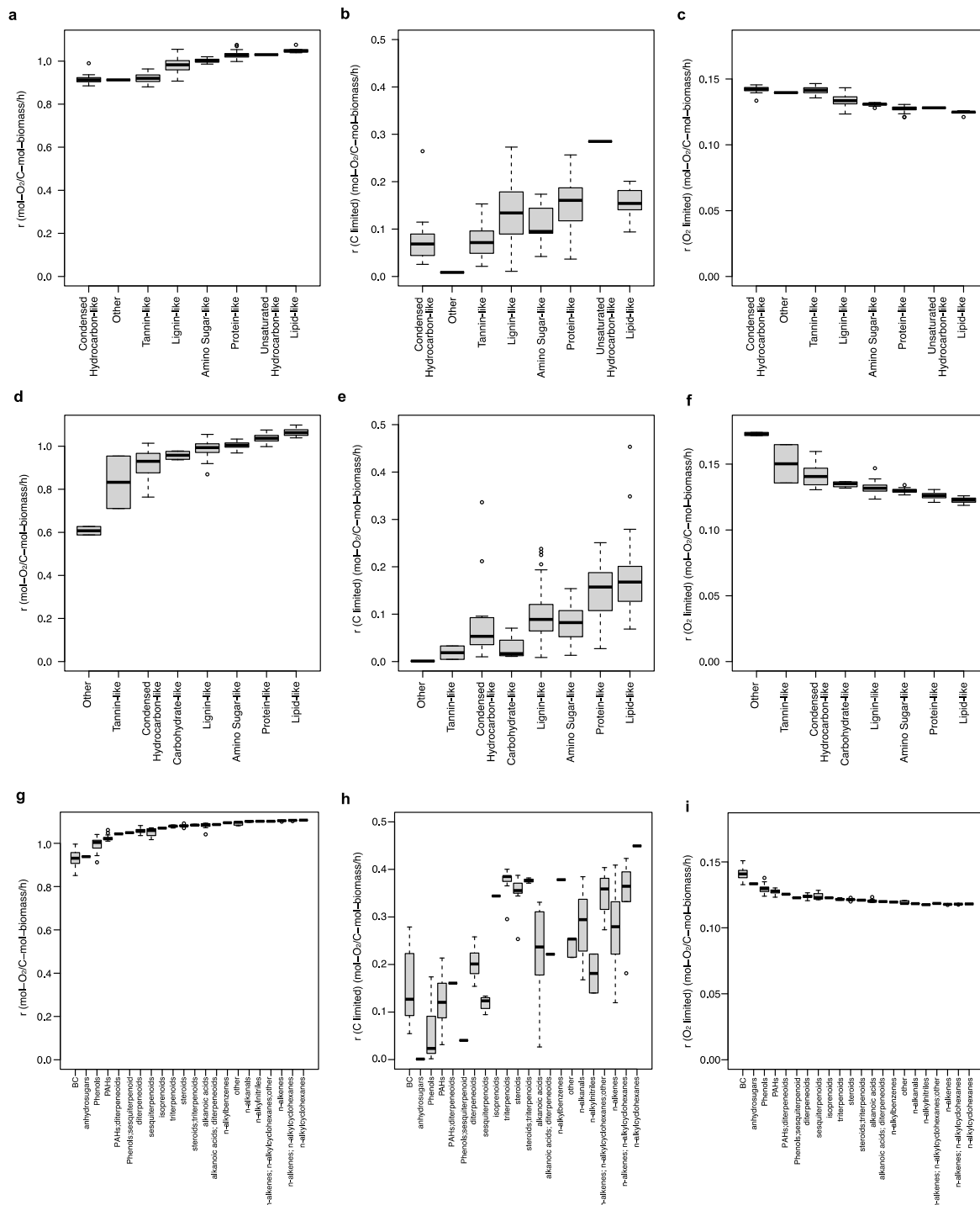
333 25th and 75th percentiles), and the upper and lower whiskers extend from the hinge to the

334 largest/smallest value no further than $1.5 * \text{IQR}$ from the hinge (where IQR is the inter-quartile

335 range, or distance between the first and third quartiles), and data beyond the end of the whiskers

336 are plotted individually.

337



338

339 **Figure S2.** Predicted metabolism of ubiquitous (a–c) surface water NOM, (d–f) sediment NOM,
 340 and (g–i) PyOM molecules, grouped by inferred chemical class or known chemical properties.

341 The first column shows predicted rates of aerobic metabolism without any elemental limitations.

342 C-limited and O₂-limited scenarios are shown in the second and third columns, respectively.

343 Median values are denoted by a bar, the lower and upper hinges correspond to the first and third

344 quartiles (the 25th and 75th percentiles), and the upper and lower whiskers extend from the hinge

345 to the largest/smallest value no further than $1.5 * \text{IQR}$ from the hinge (where IQR is the inter-

346 quartile range, or distance between the first and third quartiles), and data beyond the end of the

347 whiskers are plotted individually.

348

349 **Table S1.** PyOM molecules and chemical properties.

350

351 **Table S2.** Substrate-explicit model outputs for each PyOM compound.

352

353 **Table S3.** Substrate-explicit model outputs for each sediment NOM compound.

354

355 **Table S4.** Substrate-explicit model outputs for each surface water NOM compound.

356

357

358 SUPPORTING INFORMATION: EXTENDED MATERIALS AND METHODS

359 *Representative Pyrogenic Organic Matter (PyOM) Description*

360 To assess the bioavailability of PyOM, we searched primary literature for representative
361 compounds of the PyOM continuum. Specifically, we targeted previously characterized organic
362 compounds from field and laboratory burns of various fuel types representing a range of
363 moisture, temperature, and oxygen conditions (Table S1). The chosen compounds focused on
364 biomass burning alteration products which are often used to characterize PyOM in different
365 environmental media, such as aerosols, soils, and waters. This included compounds such as
366 theoretical BC compounds (defined here as condensed aromatic core structures polysubstituted
367 with O-containing functionalities¹), anhydrosugars, and polycyclic aromatic hydrocarbons
368 (PAHs). The list also included compounds created and/or transformed from biomass burning,
369 such as those derived from biopolymers like lignin (e.g., methoxyphenols), waxes (e.g., n-
370 alkenes from thermal dehydration of n-alkanols), and resins (e.g., thermally oxidized
371 diterpenoids).^{2,3} In total, our literature search for PyOM chemistries yielded 389 compounds
372 with 207 unique chemical formulae from 12 primary literature sources (Table S1).

373

374 *Natural Organic Matter (NOM) Description*

375 Global surface water and sediment NOM pool composition was measured with Fourier
376 transform ion cyclotron mass spectrometer (FTICR-MS) in order to be able to detected
377 thousands of OM compounds per sample, thereby providing a high-resolution perspective on
378 NOM, and the data used here are described in more detail by Garayburu-Caruso et al.⁴

379 Briefly, the WHONDRS consortium collected surface waters and sediments from 97 river
380 corridors in 8 countries within a 6-week period, from 29 July to 19 September. At each location,

381 collaborators selected sampling sites within 100 m of a station that measured river discharge,
382 height, or pressure. Surface water was collected in triplicate using a 60 mL syringe and then
383 filtered through a 0.22 μm sterivex filter (EMD Millipore) into a 40 mL glass vial (I-Chem
384 amber VOA glass vials; ThermoFisher, pre-acidified with 10 μL of 85% phosphoric acid).
385 Subsequently, 125 mL of surface sediments (1–3 cm depth) were sampled from a $\sim 1 \text{ m}^2$ area at
386 each of three depositional zone with a stainless steel scoop, making sure the sediments were
387 saturated upon collection. All samples were shipped to Pacific Northwest National Laboratory on
388 blue ice within 24 h of collection. Surface water samples were immediately frozen at $-20 \text{ }^\circ\text{C}$
389 upon receiving. Sediments were sieved to $<2 \text{ mm}$, subsampled into proteomic friendly tubes
390 (Genesee Scientific), flash frozen in liquid nitrogen and then stored at -80 until FTICR-MS
391 analysis. Note that in the methods provided by Garayburu-Caruso et al. ⁴ there is an error in the
392 description of the sediment preservation prior to FTICR-MS analysis. Corrected preservation
393 methods are used in this manuscript.

394 Prior to FTICR-MS analysis, sediment organic matter was extracted in proteomic friendly
395 tubes (Genesee Scientific) with a 1:2 ratio of sediment to water (5 g of sediment to 10 mL of
396 milli-Q water), continuously shaken in the dark at 375 rpm and $21 \text{ }^\circ\text{C}$ for 2 h. The tubes were
397 centrifuged at 6000 rcf and $21 \text{ }^\circ\text{C}$ for 5 min. The supernatant was collected and filtered through
398 0.22 μm polyethersulfone membrane filter (Millipore Sterivex, USA) into borosilicate glass
399 vials. Surface water and sediment extracts were normalized to a standardized NPOC
400 concentration of 1.5 mg C L^{-1} . Diluted samples were acidified to pH 2 with 85% phosphoric
401 acid and extracted with PPL cartridges (Bond Elut), following Dittmar et al.⁵

402 A 12 Tesla (12 T) Bruker Solarix FTICR-MS (Bruker, Solarix, Billerica, MA, USA)
403 located at the Environmental Molecular Sciences Laboratory in Richland, WA, was used to

404 collect ultrahigh-resolution mass spectra of surface water and sediment OM pools. Resolution
405 was 220 K at 481.185 m/z. The FTICR-MS was outfitted with a standard electrospray ionization
406 (ESI) source, and data were acquired in negative mode with the voltage set to +4.2 kV. The
407 instrument was externally calibrated weekly to a mass accuracy of <0.1 ppm; in addition, the
408 instrument settings were optimized by tuning on a Suwannee River Fulvic Acid (SRFA)
409 standard. Data were collected with an ion accumulation of 0.05 s for surface water and 0.1 or 0.2
410 s for sediment from 100–900 m/z at 4 M. One hundred forty-four scans were co-added for each
411 sample and internally calibrated using an OM homologous series separated by 14 Da (–CH₂
412 groups). The mass measurement accuracy was typically within 1 ppm for singly charged ions
413 across a broad m/z range (100 m/z–900 m/z). BrukerDaltonik Data Analysis (version 4.2) was
414 used to convert raw spectra to a list of m/z values by applying the FTMS peak picker module
415 with a signal-to-noise ratio (S/N) threshold set to 7 and absolute intensity threshold to the default
416 value of 100. We aligned peaks (0.5 ppm threshold) and assigned chemical formulas using
417 Formularity.⁶ The Compound Identification Algorithm in Formularity was used with the
418 following criteria: S/N > 7 and mass measurement error <0.5 ppm. This algorithm takes into
419 consideration the presence of C, H, O, N, S, and P and excludes other elements.

420 The R package “ftmsRanalysis”⁷ was used to (1) remove peaks outside of a high
421 confidence m/z range (200 m/z–900 m/z) and/or with a ¹³C isotopic signature and (2) to predict
422 chemical class assignments for each NOM molecule using oxygen-to-carbon and hydrogen-to-
423 carbon ratios (i.e., Van Krevelen classes⁸). To yield a dataset of globally ubiquitous NOM,
424 surface water and sediment NOM pools were filtered to compounds occurring in 95% of
425 samples.

426 Although FTICR-MS has the advantage of allowing for the detection of thousands of
427 NOM molecules, one drawback is that formula assignments and follow-on chemical class
428 inferences are computationally assessed rather than referenced against known standards. Because
429 of this, chemical class inferences for NOM molecules in this study are limited to a higher level of
430 molecular taxonomy than PyOM molecules that were extracted from primary literature and had
431 known compound identifications. This results in a discrepancy between compound classes
432 presented in the main text figures for NOM and PyOM molecules. We provide finer
433 classifications for PyOM compounds (e.g., phenols), many of which fall into the broader groups
434 depicted for NOM pools (e.g., lipids), to provide the maximum information we are able to infer
435 from each data type.

436

437 *Substrate-Explicit Model Description*

438 We used a substrate-explicit modelling framework developed by Song et al.⁹ to
439 characterize the bioavailability of each compound and predict its rate of decomposition. The
440 model is compound-specific and environment-agnostic (with excepted specifications of 1 bar
441 atmospheric pressure, pH 7, and 25°C), meaning that it yields predictions for each input
442 compound (as opposed to as a pool of compounds) and does not consider environmental
443 conditions such as mineralogy or redox potential. Calculation of thermodynamic functions at
444 pH=7 is important because aqueous species at pH=0 do not necessarily represent the state of
445 biological cells. Correction of Gibbs free energy for any given reaction (r) from pH=0 (ΔG_r^0) to
446 7 (ΔG_r) can be made using the following equation:

$$447 \quad \Delta G_r = \Delta G_r^0 + RTy_{H^+} \ln(10^{-7}) \quad (\text{Eq. 1})$$

448 where R is the universal gas constant [= 0.008314 kJ/(K · mol)], T is temperature in Kelvin, y_{H^+}
449 is the stoichiometric coefficient of H^+ in a given reaction. With this adjustment, the sign of Gibbs
450 free energy for an electron donor half reaction is often changed from plus to minus.

451 Three sets of organic molecules were used as model inputs: global dissolved (1) surface
452 water NOM and (2) sediment NOM pools⁴; and (3) literature-derived PyOM compounds as
453 described above. Inputs to the model were unique molecular formulae, grouped in subsequent
454 analysis by their corresponding compound classes (Table S1). If one molecular formula was
455 represented by several PyOM compounds (e.g., $C_{10}H_{16}O_2$, which corresponds to the
456 sesquiterpenoid cis-Thujan-10-oic acid and 3-, 4- substituted methylcatechol phenols), we
457 assigned multiple compound classes to that molecular formula.

458 Briefly, the substrate-explicit model uses the elemental stoichiometry of organic
459 molecules, based on molecular formulae, to predict the number of catabolic reactions that must
460 occur to provide the energy required for the synthesis of a unit carbon mole of biomass. This
461 quantity is described by the parameter lambda (λ) in which lower λ values denote more efficient
462 energetics of catabolism in producing biomass through anabolism. As described above, the
463 model also predicts the Gibbs free energy of C oxidation (ΔG_{Cox}), under standard conditions with
464 a modification to pH 7 adjusted from LaRowe and Van Cappellen¹⁰ by Song et al.⁹, as well as C
465 use efficiency (CUE) as defined by Saifuddin et al.¹¹ Lower ΔG_{Cox} denotes higher
466 thermodynamic favorability in an electron donor half reaction associated with organic matter,
467 and higher CUE reflects more C assimilated into biomass per unit C respired. We also predicted
468 the rate of aerobic metabolism (as oxygen consumed per mol-C biomass produced) under three
469 scenarios commonly observed in aquatic ecosystems: (a) C-limitation, (b) oxygen (O_2)
470 limitation, and (c) both C and O_2 -limitation. For more details of the substrate-explicit modelling

471 approach used, please see Song et al.⁹ Each metric (λ , ΔG_{Cox} , CUE, metabolic rates) denotes a
472 different aspect of bioavailability. Though the relative magnitude of the metrics in comparison to
473 each other will vary based on the specific stoichiometry of a molecule, highly bioavailable
474 compounds are indicated by low λ and ΔG_{Cox} coinciding with high CUE and metabolic rates.
475 More details on Song et al.'s substrate-explicit model are below, and we point the reader to the
476 original publication for the full methodology.

477 The substrate-explicit model used here leverages two microbial parameters [maximal
478 growth rate (μ_{max}) and harvest volume (V_h) (i.e., the volume that a microbe can access for
479 harvesting energy)] to predict OM-specific oxidative degradation pathways and reaction rates
480 based on the thermodynamic properties of OM pools. The remaining reaction kinetics are
481 formulated from the chemical formula of OM, based on thermodynamic principles. The model is
482 comprised of two major components (1) derivation of stoichiometric equations for catabolic,
483 anabolic, and metabolic reactions by combining a set of standard thermodynamic analyses^{10, 12, 13}
484 and (2) formulation of kinetic equations for the final oxidative degradation reaction of OC using
485 a relatively recent thermodynamic theory for microbial growth.¹⁴

486 For (1), we derived stoichiometric equations following the standard approaches outlined
487 in the literature.^{13, 15} Step-by-step instructions are available in Song et al. For each OM
488 compound, we derived a stoichiometric equation for oxidative degradation of OC by combining
489 catabolic (i.e., all processes for obtaining energy through substrate oxidation or other means) and
490 anabolic (i.e., synthesis of biomass using the energy provided from catabolism) reactions to
491 generate a full metabolic process. To do so, we combined two common approaches to generate
492 metabolic reactions based on stoichiometric equations—the dissipation method^{16, 17} and the
493 thermodynamic electron equivalents model (TEEM).¹² The dissipation method provides a basic

494 framework through the determination of the stoichiometric coefficient vector for metabolic
 495 reaction by coupling the catabolic and anabolic reactions based on the parameter λ , which in turn
 496 was calculated by TEEM along with dissipation energy using information on C source and its
 497 conversion into biomass. In all cases, we specified ammonium as the nitrogen source.

498 To derive kinetic equations in step (2), we use thermodynamic theory by Desmond-Le
 499 Quemener and Bouchez¹⁴ to formulate microbial growth kinetics from stoichiometric equations
 500 in step (1). In the case of oxidative degradation of OC, the microbial growth on the *i*th OC (OC_i)
 501 can be represented by

$$\mu_i = \mu^{\max} \exp\left(-\frac{|y_{OC,i}|}{V_h [OC_i]}\right) \exp\left(-\frac{|y_{O_2,i}|}{V_h [O_2]}\right)$$

502 (Eq. 2)

503 where μ_{max} is the maximal specific growth rate, V_h is the volume that a microbe can access for
 504 harvesting energy from the environment (thus termed harvest volume), $y_{OC,i}$ and y_{O_2} are the
 505 stoichiometric coefficients of OC and O₂ in the metabolic reaction associated with oxidative
 506 degradation of OC_i , and $|y_{OC,i}|$ and $|y_{O_2}|$ denote their absolute values.

507 Importantly, the model utilizes molecular formulae to predict energetic content,
 508 metabolic efficiency, and rates of aerobic metabolism, and it does not account for structural
 509 components of organic molecules (e.g., double bonds, folding patterns, cross-linkages). It also is
 510 agnostic of environmental parameters known to impact metabolic rates, such as temperature,
 511 mineral sorption, and microbial community composition. This simplified approach enables
 512 flexibility in application to high-throughput mass spectrometry techniques that yield chemical
 513 formulae but not structural information (e.g., Fourier Transform Ion Cyclotron Resonance Mass
 514 Spectrometry, FTICR-MS) and supports hypothesis generation regarding in situ molecular

515 dynamics that can be directly measured with targeted laboratory experiments. Despite its
516 limitations, the substrate-explicit model used here has proven useful in linking NOM
517 composition to aerobic metabolism in natural environments^{9, 18, 19}, and its structure is consistent
518 with Harvey et al.²⁰ who argued for the importance of thermodynamic estimates of PyOM
519 bioavailability that underlie this model. It was chosen to allow for comparison of PyOM to a
520 comprehensive assessment of global aquatic NOM pool composition.⁴

521

522 *Statistics and Data Availability*

523 We compared modelling outputs from representative PyOM to outputs of ubiquitous
524 NOM pools to infer relative bioavailability using ANOVA and Tukey HSD statistical tests with
525 R software. All model outputs are available in Tables S2-S4. Code is available at:
526 <https://github.com/hyunseobsong/lambda>. Data describing NOM pool chemistry are published as
527 a data package²¹ (available at: doi:10.15485/1729719) and are discussed in more detail by
528 Garayburu-Caruso et al.⁴

529

530

531 **References.**

- 532
- 533 1. Wagner, S.; Ding, Y.; Jaffé, R., A new perspective on the apparent solubility of dissolved
534 black carbon. *Frontiers in Earth Science* **2017**, *5*, 75.
- 535 2. Oros, D. R.; Simoneit, B. R., Identification and emission factors of molecular tracers in
536 organic aerosols from biomass burning Part 1. Temperate climate conifers. *Applied*
537 *Geochemistry* **2001**, *16*, (13), 1513-1544.
- 538 3. Oros, D. R.; Simoneit, B. R., Identification and emission factors of molecular tracers in
539 organic aerosols from biomass burning Part 2. Deciduous trees. *Applied Geochemistry* **2001**, *16*,
540 (13), 1545-1565.
- 541 4. Garayburu-Caruso, V. A.; Danczak, R. E.; Stegen, J. C.; Renteria, L.; Mccall, M.;
542 Goldman, A. E.; Chu, R. K.; Toyoda, J.; Resch, C. T.; Torgeson, J. M., Using Community
543 Science to Reveal the Global Chemogeography of River Metabolomes. *Metabolites* **2020**, *10*,
544 (12), 518.
- 545 5. Dittmar, T.; Koch, B.; Hertkorn, N.; Kattner, G., A simple and efficient method for the
546 solid-phase extraction of dissolved organic matter (SPE-DOM) from seawater. *Limnology and*
547 *Oceanography: Methods* **2008**, *6*, (6), 230-235.
- 548 6. Tolić, N.; Liu, Y.; Liyu, A.; Shen, Y.; Tfaily, M. M.; Kujawinski, E. B.; Longnecker, K.;
549 Kuo, L.-J.; Robinson, E. W.; Paša-Tolić, L., Formularity: software for automated formula
550 assignment of natural and other organic matter from ultrahigh-resolution mass spectra. *Analytical*
551 *chemistry* **2017**, *89*, (23), 12659-12665.
- 552 7. Bramer, L. M.; White, A. M.; Stratton, K. G.; Thompson, A. M.; Claborne, D.;
553 Hofmockel, K.; McCue, L. A., ftmsRanalysis: An R package for exploratory data analysis and
554 interactive visualization of FT-MS data. *PLoS computational biology* **2020**, *16*, (3), e1007654.
- 555 8. Kim, S.; Kaplan, L. A.; Benner, R.; Hatcher, P. G., Hydrogen-deficient molecules in
556 natural riverine water samples—evidence for the existence of black carbon in DOM. *Marine*
557 *Chemistry* **2004**, *92*, (1-4), 225-234.
- 558 9. Song, H.-S.; Stegen, J. C.; Graham, E. B.; Lee, J.-Y.; Garayburu-Caruso, V.; Nelson, W.
559 C.; Chen, X.; Moulton, J. D.; Scheibe, T. D., Representing Organic Matter Thermodynamics in
560 Biogeochemical Reactions via Substrate-Explicit Modeling. *Frontiers in Microbiology* **2020**.
- 561 10. LaRowe, D. E.; Van Cappellen, P., Degradation of natural organic matter: a
562 thermodynamic analysis. *Geochimica et Cosmochimica Acta* **2011**, *75*, (8), 2030-2042.
- 563 11. Saifuddin, M.; Bhatnagar, J. M.; Segrè, D.; Finzi, A. C., Microbial carbon use efficiency
564 predicted from genome-scale metabolic models. *Nature communications* **2019**, *10*, (1), 1-10.
- 565 12. McCarty, P. L., Thermodynamic electron equivalents model for bacterial yield
566 prediction: modifications and comparative evaluations. *Biotechnology and bioengineering* **2007**,
567 *97*, (2), 377-388.
- 568 13. Kleerebezem, R.; Van Loosdrecht, M. C., A generalized method for thermodynamic state
569 analysis of environmental systems. *Critical Reviews in Environmental Science and Technology*
570 **2010**, *40*, (1), 1-54.
- 571 14. Desmond-Le Quéméner, E.; Bouchez, T., A thermodynamic theory of microbial growth.
572 *The ISME journal* **2014**, *8*, (8), 1747-1751.
- 573 15. Rittmann, B. E.; McCarty, P. L., *Environmental biotechnology: principles and*
574 *applications*. McGraw-Hill Education: 2001.

- 575 16. Hoiijnen, J.; van Loosdrecht, M. C.; Tijhuis, L., A black box mathematical model to
576 calculate auto-and heterotrophic biomass yields based on Gibbs energy dissipation.
577 *Biotechnology and bioengineering* **1992**, *40*, (10), 1139-1154.
- 578 17. Heijnen, J.; Van Dijken, J., Response to comments on “in search of a thermodynamic
579 description of biomass yields for the chemotropic growth of microorganisms”. *Biotechnology*
580 *and Bioengineering* **1993**, *42*, (9), 1127-1130.
- 581 18. Graham, E. B.; Tfaily, M. M.; Crump, A. R.; Goldman, A. E.; Bramer, L. M.; Arntzen,
582 E.; Romero, E.; Resch, C. T.; Kennedy, D. W.; Stegen, J. C., Carbon inputs from riparian
583 vegetation limit oxidation of physically bound organic carbon via biochemical and
584 thermodynamic processes. *Journal of Geophysical Research: Biogeosciences* **2017**, *122*, (12),
585 3188-3205.
- 586 19. Garayburu-Caruso, V. A.; Stegen, J. C.; Song, H.-S.; Renteria, L.; Wells, J.; Garcia, W.;
587 Resch, C. T.; Goldman, A. E.; Chu, R. K.; Toyoda, J.; Graham, E. B., Carbon limitation leads to
588 thermodynamic regulation of aerobic metabolism. *Environmental Science & Technology Letters*
589 **2020**, *7*, 517-524.
- 590 20. Harvey, O. R.; Myers-Pigg, A. N.; Kuo, L.-J.; Singh, B. P.; Kuehn, K. A.; Louchouart,
591 P., Discrimination in degradability of soil pyrogenic organic matter follows a return-on-energy-
592 investment principle. *Environmental science & technology* **2016**, *50*, (16), 8578-8585.
- 593 21. Goldman, A. E.; Chu, R. K.; Danczak, R. E.; Daly, R. A.; Fansler, S.; Garayburu-Caruso,
594 V. A.; Graham, E. B.; McCall, M. L.; Ren, H.; Renteria, L. *WHONDRS Summer 2019 Sampling*
595 *Campaign: Global River Corridor Sediment FTICR-MS, NPOC, and Aerobic Respiration*;
596 Environmental System Science Data Infrastructure for a Virtual Ecosystem ...: 2020.
597
598

599

600

601 REFERENCES

- 602 1. Bladon, K. D.; Emelko, M. B.; Silins, U.; Stone, M., Wildfire and the future of water
603 supply. In ACS Publications: 2014.
- 604 2. Shakesby, R.; Doerr, S., Wildfire as a hydrological and geomorphological agent. *Earth-*
605 *Science Reviews* **2006**, *74*, (3-4), 269-307.
- 606 3. Randerson, J. T.; Liu, H.; Flanner, M. G.; Chambers, S. D.; Jin, Y.; Hess, P. G.; Pfister,
607 G.; Mack, M.; Treseder, K.; Welp, L., The impact of boreal forest fire on climate warming.
608 *science* **2006**, *314*, (5802), 1130-1132.
- 609 4. Verma, S.; Jayakumar, S., Impact of forest fire on physical, chemical and biological
610 properties of soil: A review. *Proceedings of the International Academy of Ecology and*
611 *Environmental Sciences* **2012**, *2*, (3), 168.
- 612 5. Smith, H. G.; Sheridan, G. J.; Lane, P. N.; Nyman, P.; Haydon, S., Wildfire effects on
613 water quality in forest catchments: a review with implications for water supply. *Journal of*
614 *Hydrology* **2011**, *396*, (1-2), 170-192.
- 615 6. Krawchuk, M. A.; Moritz, M. A., Constraints on global fire activity vary across a
616 resource gradient. *Ecology* **2011**, *92*, (1), 121-132.
- 617 7. Pierce, J. L.; Meyer, G. A.; Jull, A. T., Fire-induced erosion and millennial-scale climate
618 change in northern ponderosa pine forests. *Nature* **2004**, *432*, (7013), 87.
- 619 8. Abatzoglou, J. T.; Juang, C. S.; Williams, A. P.; Kolden, C. A.; Westerling, A. L.,
620 Increasing synchronous fire danger in forests of the western United States. *Geophysical*
621 *Research Letters* **2021**, *48*, (2), e2020GL091377.
- 622 9. Bowman, D. M.; Kolden, C. A.; Abatzoglou, J. T.; Johnston, F. H.; van der Werf, G. R.;
623 Flannigan, M., Vegetation fires in the Anthropocene. *Nature Reviews Earth & Environment*
624 **2020**, *1*, (10), 500-515.
- 625 10. Flannigan, M. D.; Krawchuk, M. A.; de Groot, W. J.; Wotton, B. M.; Gowman, L. M.,
626 Implications of changing climate for global wildland fire. *International journal of wildland fire*
627 **2009**, *18*, (5), 483-507.
- 628 11. Wagner, S.; Jaffé, R.; Stubbins, A., Dissolved black carbon in aquatic ecosystems.
629 *Limnology and Oceanography Letters* **2018**, *3*, (3), 168-185.
- 630 12. Abney, R. B.; Kuhn, T. J.; Chow, A.; Hockaday, W.; Fogel, M. L.; Berhe, A. A.,
631 Pyrogenic carbon erosion after the Rim Fire, Yosemite National Park: The role of burn severity
632 and slope. *Journal of Geophysical Research: Biogeosciences* **2019**, *124*, (2), 432-449.
- 633 13. Wozniak, A. S.; Goranov, A. I.; Mitra, S.; Bostick, K. W.; Zimmerman, A. R.;
634 Schlesinger, D. R.; Myneni, S.; Hatcher, P. G., Molecular heterogeneity in pyrogenic dissolved
635 organic matter from a thermal series of oak and grass chars. *Organic Geochemistry* **2020**, *148*,
636 104065.
- 637 14. Masiello, C. A., New directions in black carbon organic geochemistry. *Marine Chemistry*
638 **2004**, *92*, (1-4), 201-213.
- 639 15. Wagner, S.; Coppola, A. I.; Stubbins, A.; Dittmar, T.; Niggemann, J.; Drake, T. W.;
640 Seidel, M.; Spencer, R. G.; Bao, H., Questions remain about the biolability of dissolved black
641 carbon along the combustion continuum. *Nature communications* **2021**, *12*, (1), 1-4.
- 642 16. Jaffé, R.; Ding, Y.; Niggemann, J.; Vähätalo, A. V.; Stubbins, A.; Spencer, R. G.;
643 Campbell, J.; Dittmar, T., Global charcoal mobilization from soils via dissolution and riverine
644 transport to the oceans. *Science* **2013**, *340*, (6130), 345-347.

- 645 17. Santin, C.; Doerr, S. H.; Kane, E. S.; Masiello, C. A.; Ohlson, M.; de la Rosa, J. M.;
646 Preston, C. M.; Dittmar, T., Towards a global assessment of pyrogenic carbon from vegetation
647 fires. *Global Change Biology* **2016**, *22*, (1), 76-91.
- 648 18. Dittmar, T.; De Rezende, C. E.; Manecki, M.; Niggemann, J.; Ovalle, A. R. C.; Stubbins,
649 A.; Bernardes, M. C., Continuous flux of dissolved black carbon from a vanished tropical forest
650 biome. *Nature Geoscience* **2012**, *5*, (9), 618-622.
- 651 19. Hockaday, W. C.; Grannas, A. M.; Kim, S.; Hatcher, P. G., The transformation and
652 mobility of charcoal in a fire-impacted watershed. *Geochimica et Cosmochimica Acta* **2007**, *71*,
653 (14), 3432-3445.
- 654 20. Santín, C.; Doerr, S. H.; Kane, E. S.; Masiello, C. A.; Ohlson, M.; de la Rosa, J. M.;
655 Preston, C. M.; Dittmar, T., Towards a global assessment of pyrogenic carbon from vegetation
656 fires. *Global Change Biology* **2016**, *22*, (1), 76-91.
- 657 21. Emelko, M. B.; Silins, U.; Bladon, K. D.; Stone, M., Implications of land disturbance on
658 drinking water treatability in a changing climate: Demonstrating the need for “source water
659 supply and protection” strategies. *Water research* **2011**, *45*, (2), 461-472.
- 660 22. Hohner, A. K.; Terry, L. G.; Townsend, E. B.; Summers, R. S.; Rosario-Ortiz, F. L.,
661 Water treatment process evaluation of wildfire-affected sediment leachates. *Environmental*
662 *Science: Water Research & Technology* **2017**, *3*, (2), 352-365.
- 663 23. Meyer, G. A.; Wells, S. G., Fire-related sedimentation events on alluvial fans,
664 Yellowstone National Park, USA. *Journal of Sedimentary Research* **1997**, *67*, (5), 776-791.
- 665 24. Elliott, J. G.; Parker, R., Developing a post-fire flood chronology and recurrence
666 probability from alluvial stratigraphy in the Buffalo Creek watershed, Colorado, USA.
667 *Hydrological Processes* **2001**, *15*, (15), 3039-3051.
- 668 25. Bigio, E.; Swetnam, T. W.; Baisan, C. H., A comparison and integration of tree-ring and
669 alluvial records of fire history at the Missionary Ridge Fire, Durango, Colorado, USA. *The*
670 *Holocene* **2010**, *20*, (7), 1047-1061.
- 671 26. Kuzyakov, Y.; Bogomolova, I.; Glaser, B., Biochar stability in soil: decomposition
672 during eight years and transformation as assessed by compound-specific ¹⁴C analysis. *Soil*
673 *Biology and Biochemistry* **2014**, *70*, 229-236.
- 674 27. Masiello, C.; Druffel, E., Organic and black carbon ¹³C and ¹⁴C through the Santa
675 Monica Basin sediment oxic-anoxic transition. *Geophysical research letters* **2003**, *30*, (4).
- 676 28. Masiello, C.; Louchouart, P., Fire in the ocean. *Science* **2013**, *340*, (6130), 287-288.
- 677 29. Myers-Pigg, A. N.; Louchouart, P.; Amon, R. M.; Prokushkin, A.; Pierce, K.; Rubtsov,
678 A., Labile pyrogenic dissolved organic carbon in major Siberian Arctic rivers: Implications for
679 wildfire-stream metabolic linkages. *Geophysical Research Letters* **2015**, *42*, (2), 377-385.
- 680 30. Norwood, M. J.; Louchouart, P.; Kuo, L.-J.; Harvey, O. R., Characterization and
681 biodegradation of water-soluble biomarkers and organic carbon extracted from low temperature
682 chars. *Organic Geochemistry* **2013**, *56*, 111-119.
- 683 31. Zimmerman, A. R.; Ouyang, L., Priming of pyrogenic C (biochar) mineralization by
684 dissolved organic matter and vice versa. *Soil Biology and Biochemistry* **2019**, *130*, 105-112.
- 685 32. Sohi, S. P.; Krull, E.; Lopez-Capel, E.; Bol, R., A review of biochar and its use and
686 function in soil. *Advances in agronomy* **2010**, *105*, 47-82.
- 687 33. Mia, S.; Dijkstra, F. A.; Singh, B., Long-term aging of biochar: a molecular
688 understanding with agricultural and environmental implications. *Advances in agronomy* **2017**,
689 *141*, 1-51.

- 690 34. Song, H.-S.; Stegen, J. C.; Graham, E. B.; Lee, J.-Y.; Garayburu-Caruso, V.; Nelson, W.
691 C.; Chen, X.; Moulton, J. D.; Scheibe, T. D., Representing Organic Matter Thermodynamics in
692 Biogeochemical Reactions via Substrate-Explicit Modeling. *Frontiers in Microbiology* **2020**.
- 693 35. Arndt, S.; Jørgensen, B. B.; LaRowe, D. E.; Middelburg, J.; Pancost, R.; Regnier, P.,
694 Quantifying the degradation of organic matter in marine sediments: a review and synthesis.
695 *Earth-science reviews* **2013**, *123*, 53-86.
- 696 36. Wagner, S.; Ding, Y.; Jaffé, R., A new perspective on the apparent solubility of dissolved
697 black carbon. *Frontiers in Earth Science* **2017**, *5*, 75.
- 698 37. Oros, D. R.; Simoneit, B. R., Identification and emission factors of molecular tracers in
699 organic aerosols from biomass burning Part 1. Temperate climate conifers. *Applied*
700 *Geochemistry* **2001**, *16*, (13), 1513-1544.
- 701 38. Oros, D. R.; Simoneit, B. R., Identification and emission factors of molecular tracers in
702 organic aerosols from biomass burning Part 2. Deciduous trees. *Applied Geochemistry* **2001**, *16*,
703 (13), 1545-1565.
- 704 39. Graham, E. B.; Tfaily, M. M.; Crump, A. R.; Goldman, A. E.; Bramer, L. M.; Arntzen,
705 E.; Romero, E.; Resch, C. T.; Kennedy, D. W.; Stegen, J. C., Carbon inputs from riparian
706 vegetation limit oxidation of physically bound organic carbon via biochemical and
707 thermodynamic processes. *Journal of Geophysical Research: Biogeosciences* **2017**, *122*, (12),
708 3188-3205.
- 709 40. Garayburu-Caruso, V. A.; Stegen, J. C.; Song, H.-S.; Renteria, L.; Wells, J.; Garcia, W.;
710 Resch, C. T.; Goldman, A. E.; Chu, R. K.; Toyoda, J.; Graham, E. B., Carbon limitation leads to
711 thermodynamic regulation of aerobic metabolism. *Environmental Science & Technology Letters*
712 **2020**, *7*, 517-524.
- 713 41. Harvey, O. R.; Myers-Pigg, A. N.; Kuo, L.-J.; Singh, B. P.; Kuehn, K. A.; Louchouart,
714 P., Discrimination in degradability of soil pyrogenic organic matter follows a return-on-energy-
715 investment principle. *Environmental science & technology* **2016**, *50*, (16), 8578-8585.
- 716 42. Garayburu-Caruso, V. A.; Danczak, R. E.; Stegen, J. C.; Renteria, L.; McCall, M.;
717 Goldman, A. E.; Chu, R. K.; Toyoda, J.; Resch, C. T.; Torgeson, J. M., Using Community
718 Science to Reveal the Global Chemogeography of River Metabolomes. *Metabolites* **2020**, *10*,
719 (12), 518.
- 720 43. LaRowe, D. E.; Van Cappellen, P., Degradation of natural organic matter: a
721 thermodynamic analysis. *Geochimica et Cosmochimica Acta* **2011**, *75*, (8), 2030-2042.
- 722 44. Saifuddin, M.; Bhatnagar, J. M.; Segrè, D.; Finzi, A. C., Microbial carbon use efficiency
723 predicted from genome-scale metabolic models. *Nature communications* **2019**, *10*, (1), 1-10.
- 724 45. Goldman, A. E.; Chu, R. K.; Danczak, R. E.; Daly, R. A.; Fansler, S.; Garayburu-Caruso,
725 V. A.; Graham, E. B.; McCall, M. L.; Ren, H.; Renteria, L. *WHONDRS Summer 2019 Sampling*
726 *Campaign: Global River Corridor Sediment FTICR-MS, NPOC, and Aerobic Respiration*;
727 Environmental System Science Data Infrastructure for a Virtual Ecosystem ...: 2020.
- 728 46. Harvey, O. R.; Kuo, L.-J.; Zimmerman, A. R.; Louchouart, P.; Amonette, J. E.; Herbert,
729 B. E., An index-based approach to assessing recalcitrance and soil carbon sequestration potential
730 of engineered black carbons (biochars). *Environmental science & technology* **2012**, *46*, (3),
731 1415-1421.
- 732 47. Cawley, K. M.; Hohner, A. K.; McKee, G. A.; Borch, T.; Omur-Ozbek, P.; Oropeza, J.;
733 Rosario-Ortiz, F. L., Characterization and spatial distribution of particulate and soluble carbon
734 and nitrogen from wildfire-impacted sediments. *Journal of soils and sediments* **2018**, *18*, (4),
735 1314-1326.

- 736 48. Hohner, A. K.; Rhoades, C. C.; Wilkerson, P.; Rosario-Ortiz, F. L., Wildfires Alter
737 Forest Watersheds and Threaten Drinking Water Quality. *Accounts of chemical research* **2019**.
- 738 49. Domeignoz-Horta, L. A.; Pold, G.; Liu, X.-J. A.; Frey, S. D.; Melillo, J. M.; DeAngelis,
739 K. M., Microbial diversity drives carbon use efficiency in a model soil. *Nature communications*
740 **2020**, *11*, (1), 1-10.
- 741 50. Pold, G.; Domeignoz-Horta, L. A.; Morrison, E. W.; Frey, S. D.; Sistla, S. A.; DeAngelis,
742 K. M., Carbon use efficiency and its temperature sensitivity covary in soil bacteria. *Mbio* **2020**,
743 *11*, (1).
- 744 51. Wagner, S.; Dittmar, T.; Jaffé, R., Molecular characterization of dissolved black nitrogen
745 via electrospray ionization Fourier transform ion cyclotron resonance mass spectrometry.
746 *Organic Geochemistry* **2015**, *79*, 21-30.
- 747 52. Neary, D. G.; Ryan, K. C.; DeBano, L. F., Wildland fire in ecosystems: effects of fire on
748 soils and water. *Gen. Tech. Rep. RMRS-GTR-42-vol. 4. Ogden, UT: US Department of*
749 *Agriculture, Forest Service, Rocky Mountain Research Station. 250 p.* **2005**, 42.
- 750 53. Wang, G.; Jagadamma, S.; Mayes, M. A.; Schadt, C. W.; Steinweg, J. M.; Gu, L.; Post,
751 W. M., Microbial dormancy improves development and experimental validation of ecosystem
752 model. *The ISME journal* **2015**, *9*, (1), 226-237.
- 753 54. Abramoff, R.; Xu, X.; Hartman, M.; O'Brien, S.; Feng, W.; Davidson, E.; Finzi, A.;
754 Moorhead, D.; Schimel, J.; Torn, M., The Millennial model: in search of measurable pools and
755 transformations for modeling soil carbon in the new century. *Biogeochemistry* **2018**, *137*, (1-2),
756 51-71.
- 757 55. Moorhead, D. L.; Lashermes, G.; Sinsabaugh, R. L., A theoretical model of C-and N-
758 acquiring exoenzyme activities, which balances microbial demands during decomposition. *Soil*
759 *Biology and Biochemistry* **2012**, *53*, 133-141.
- 760 56. Sulman, B. N.; Shevliakova, E.; Brzostek, E. R.; Kivlin, S. N.; Malyshev, S.; Menge, D.
761 N.; Zhang, X., Diverse mycorrhizal associations enhance terrestrial C storage in a global model.
762 *Global Biogeochemical Cycles* **2019**, *33*, (4), 501-523.
- 763 57. Wieder, W. R.; Cleveland, C. C.; Smith, W. K.; Todd-Brown, K., Future productivity and
764 carbon storage limited by terrestrial nutrient availability. *Nature Geoscience* **2015**, *8*, (6), 441-
765 444.
- 766 58. Graham, E. B.; Hofmockel, K., A new frontier in molecular applications of ecological
767 stoichiometry to understand global soil organic matter decomposition. *EcoEvoRxiv* **2021**.
- 768 59. Song, H.-S.; Stegen, J. C.; Graham, E. B.; Lee, J.-Y.; Garayburu-Caruso, V.; Nelson, W.
769 C.; Chen, X.; Moulton, J. D.; Scheibe, T. D., Representing Organic Matter Thermodynamics in
770 Biogeochemical Reactions via Substrate-Explicit Modeling. *bioRxiv* **2020**.
- 771 60. Santin, C.; Doerr, S. H.; Jones, M. W.; Merino, A.; Warneke, C.; Roberts, J. M., The
772 relevance of pyrogenic carbon for carbon budgets from fires: insights from the FIREX
773 experiment. *Global Biogeochemical Cycles* **2020**, *34*, (9), e2020GB006647.
- 774 61. Thevenot, M.; Dignac, M.-F.; Rumpel, C., Fate of lignins in soils: a review. *Soil Biology*
775 *and Biochemistry* **2010**, *42*, (8), 1200-1211.
- 776 62. Ward, N. D.; Keil, R. G.; Medeiros, P. M.; Brito, D. C.; Cunha, A. C.; Dittmar, T.;
777 Yager, P. L.; Krusche, A. V.; Richey, J. E., Degradation of terrestrially derived macromolecules
778 in the Amazon River. *Nature Geoscience* **2013**, *6*, (7), 530-533.
- 779 63. Bushnell, L.; Haas, H., The utilization of certain hydrocarbons by microorganisms.
780 *Journal of Bacteriology* **1941**, *41*, (5), 653.

- 781 64. Pozdnyakova, N. N., Involvement of the ligninolytic system of white-rot and litter-
782 decomposing fungi in the degradation of polycyclic aromatic hydrocarbons. *Biotechnology*
783 *research international* **2012**, 2012.
- 784 65. Rabus, R.; Boll, M.; Heider, J.; Meckenstock, R. U.; Buckel, W.; Einsle, O.; Ermler, U.;
785 Golding, B. T.; Gunsalus, R. P.; Kroneck, P. M., Anaerobic microbial degradation of
786 hydrocarbons: from enzymatic reactions to the environment. *Journal of molecular microbiology*
787 *and biotechnology* **2016**, 26, (1-3), 5-28.
- 788 66. Coates, J. D.; Woodward, J.; Allen, J.; Philp, P.; Lovley, D. R., Anaerobic degradation of
789 polycyclic aromatic hydrocarbons and alkanes in petroleum-contaminated marine harbor
790 sediments. *Applied and Environmental Microbiology* **1997**, 63, (9), 3589-3593.
- 791 67. Knicker, H., "Black nitrogen"—an important fraction in determining the recalcitrance of
792 charcoal. *Organic Geochemistry* **2010**, 41, (9), 947-950.
- 793 68. de la Rosa, J. M.; Knicker, H., Bioavailability of N released from N-rich pyrogenic
794 organic matter: an incubation study. *Soil Biology and Biochemistry* **2011**, 43, (12), 2368-2373.
- 795 69. Wiesenberg, G. L.; Schwarzbauer, J.; Schmidt, M. W.; Schwark, L., Source and turnover
796 of organic matter in agricultural soils derived from n-alkane/n-carboxylic acid compositions and
797 C-isotope signatures. *Organic Geochemistry* **2004**, 35, (11-12), 1371-1393.
- 798 70. Smittenberg, R. H.; Hopmans, E. C.; Schouten, S.; Hayes, J. M.; Eglinton, T. I.;
799 Sinninghe Damsté, J., Compound-specific radiocarbon dating of the varved Holocene
800 sedimentary record of Saanich Inlet, Canada. *Paleoceanography* **2004**, 19, (2).
- 801 71. Knicker, H.; Hilscher, A.; De la Rosa, J.; González-Pérez, J. A.; González-Vila, F. J.,
802 Modification of biomarkers in pyrogenic organic matter during the initial phase of charcoal
803 biodegradation in soils. *Geoderma* **2013**, 197, 43-50.
- 804 72. Grossi, V.; Cravo-Laureau, C.; Guyoneaud, R.; Ranchou-Peyruse, A.; Hirschler-Réa, A.,
805 Metabolism of n-alkanes and n-alkenes by anaerobic bacteria: A summary. *Organic*
806 *Geochemistry* **2008**, 39, (8), 1197-1203.
- 807 73. Colby, J.; Stirling, D. I.; Dalton, H., The soluble methane mono-oxygenase of
808 *Methylococcus capsulatus* (Bath). Its ability to oxygenate n-alkanes, n-alkenes, ethers, and
809 alicyclic, aromatic and heterocyclic compounds. *Biochemical Journal* **1977**, 165, (2), 395-402.
- 810 74. Wilkes, H.; Buckel, W.; Golding, B. T.; Rabus, R., Metabolism of hydrocarbons in n-
811 alkane-utilizing anaerobic bacteria. *Journal of molecular microbiology and biotechnology* **2016**,
812 26, (1-3), 138-151.
- 813 75. Mbadanga, S. M.; Wang, L.-Y.; Zhou, L.; Liu, J.-F.; Gu, J.-D.; Mu, B.-Z., Microbial
814 communities involved in anaerobic degradation of alkanes. *International Biodeterioration &*
815 *Biodegradation* **2011**, 65, (1), 1-13.
- 816 76. Yongdong, Z.; Yaling, S.; Zhengwen, L.; Xiangchao, C.; Jinlei, Y.; Xiaodan, D.; Miao,
817 J., Long-chain n-alkenes in recent sediment of Lake Lugu (SW China) and their ecological
818 implications. *Limnologia* **2015**, 52, 30-40.
- 819 77. Canuel, E. A.; Martens, C. S., Reactivity of recently deposited organic matter:
820 Degradation of lipid compounds near the sediment-water interface. *Geochimica et cosmochimica*
821 *acta* **1996**, 60, (10), 1793-1806.
- 822 78. Bacik, J. P.; Jarboe, L. R., Bioconversion of anhydrosugars: emerging concepts and
823 strategies. *IUBMB life* **2016**, 68, (9), 700-708.
- 824 79. Suciú, L. G.; Masiello, C. A.; Griffin, R. J., Anhydrosugars as tracers in the Earth system.
825 *Biogeochemistry* **2019**, 146, (3), 209-256.

- 826 80. Abiven, S.; Santin, C., From Fires to Oceans: Dynamics of Fire-Derived Organic Matter
827 in Terrestrial and Aquatic Ecosystems. *Frontiers in Earth Science* **2019**, *7*, 31.
- 828 81. Zimmerman, A. R.; Mitra, S., Trial by fire: on the terminology and methods used in
829 pyrogenic organic carbon research. *Frontiers in Earth Science* **2017**, *5*, 95.
830